UBC Rapid

Induction Extruder - Operational Model

v1.1.0

Principal Authors:

Jacob Bayless

Steve Novakov

Vicky Wang

July 5, 2013

Contents

1 Introduction

This document outlines the derivation and implementation of the physical model behind the induction heating extruder being developed by UBC Rapid. The development of this extruder is motivated by the desire for increased temperature control in the extrusion of thermoplastics in a rapid prototyping platform such as RepRap Darwin, Mendel, Prusa Mendel and MendelMax. Many common thermoplastic extruders are based around a motor-controlled roller, which feeds a thermoplastic filament through the nozzle, and a heating element to melt the thermoplastic near the application tip. Existing nichrome heating solutions tend to create a large distribution of heat in the extruder nozzle, thereby increasing the volume of liquid thermoplastic filament. This reduces the accuracy of the feeding system, by creating disparity between the desired and actual amount of material being pushed through the nozzle tip by the rollers. Assuming that a fairly accurate motion control system is in place, (COMMENT ABOUT MOTION RESOLUTION OF PRUSA MENDEL), this disparity is a significant bottleneck in attaining finer printing resolutions. Using a high frequency driving coil wrapped around a glass nozzle, a small ring target of desireable geometry and material can be embedded in the nozzle and heated to high temperatures while maintaning a small, localized distribution of heat. The smaller heat distribution of the induction extruder aids in keeping the majority of the filament in the nozzle solid, thereby increasing the accuracy of the feeding system.

Rather than a scientific paper, this document is written somewhat as a guide. While not as concrete as a dedicated hardware specification, it serves to guide readers with a basic understanding of electromagnetics and, at minimum, 2nd year university mathematics, into designing their own induction heating system, whether for thermoplastic extrusion or otherwise.

2 Model Outline

The Induction Heating Extruder can be modeled with the following basic components:

- **Driver coil** - Large inductor coil, physically wrapped around the nozzle and inudction target assembly.
- **Nozzle** - Extrusion nozzle, must be an insulating material. The lower the coefficient of thermal conductivity, the more localized the temperature gradient will be, with respect to the induction target. Candidate materials include glass, or insulating ceramics such as porcelain.
- **Induction Target** - Conductive ring, with preferably high magnetic permeability, in which heat is produced from induced friction from rapidly alternating eddy currents.
- **Electromagnetic Shield (Optional)** - Optional shield to increase power transfer to target, (lower leakage inductance from driver coil, higher efficiency).

This model implements an approach based on continuous time differential equations and carefully defined boundary conditions which work well with the simple geometries currently in use. Future implementations which could have more complex target geometries may rely on a finite element approach.

2.1 Geometry

The basic electromagnetic model of the extruder consists of a driver coil, internal heating target, nozzle housing and an, (optional), electromagnetic shield. In the case of extrusion, the target must be a shape with a center void for the thermoplastic to flow through. Due to the symmetry of the internal magnetic field, the most optimal shape is likely toroidal or cylindrical, such as that shown in Figure 1. The exact shape of the induction target, (z = f(s) in Figure 1), can be determined based on desired operational characteristics and the current in the driver coil. The majority of the mathematics presented is in cylindrical coordinates. Even non-ideal

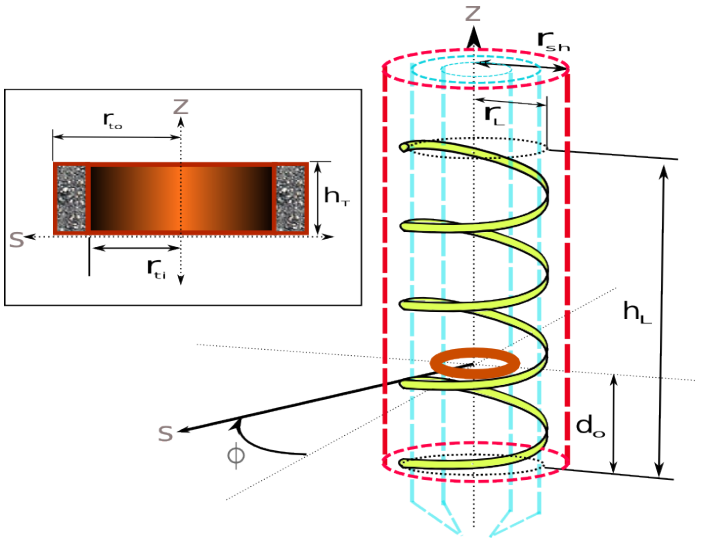

Figure 1: Geometrical definitions for basic induction extruder system. Induction target, (orange), is cocentric with driver coil. The spacing of the coil loops is exaggerated to illustrate inner structures.

solenoids typically have a high degree of symmetry in the radial coordinate, ϕ, and solving the field equations this way is less convoluted than in cartesian coordinates. This operational model also assumes insignificant changes in field strength with respect to the vertical coordinate, at least in the region immediately surrounding the induction target.

2.2 Physical Parameters

The physical parameters of this generic model are any relevant characteristics which are required to calculate the voltage response in the driver coil from the coupling of the heating target. These parameters are summarized in Table 1.

2.3 Boundaries and Regions

This document uses the notation $\mathcal{R}_i$ to label the cylindrical section of space in region i.

Table 1: Required parameters for operational model.

Component	Parameter	Description
Driver Coil	r_L	Nominal radius.
	t_L	Coil wire thickness.
	h_L	Total coil height.
	N_L	Number of turns in driver coil. Turns are assumed to be evenly spaced in majority of cases.
	k_c	Thermal conductivity of coil material, $W/(m\dot{K})$
	d_o	Vertical offset of coil with respect to target center.
Nozzle	k_n	Thermal conductivity of nozzle material, in $W/(m\dot{K})$.
	$\epsilon_{r,n}$	Relative electric permittivity of nozzle material.
	$\mu_{r,n}$	Relative magnetic permeability of nozzle material.
Target	r_{to}	Outer limit of target geometry.
	r_{ti}	Inner limit of target geometry.
	h_T	Target height in $\vec{z}$.
	ϵ_T	Target electrical permittivity.
	μ_T	Target magnetic permeability.
	σ_T	Electrical conductivity of target.
	k_T	Thermal conductivity of target material, in $W/(m\dot{K})$.
Insulation Material	ϵ_I	Inner radius of electromagnetic shield.
	μ_I	Thickness of electromagnetic shield.
Electromagnetic Shield	r_{shi}	Inner radius of electromagnetic shield.
	σ_S	Electrical conductivity of electromagnetic shield.
	t_s	Thickness of electromagnetic shield.

Table 2: Full set of regions of electromagnetic wave propagation in operational model. Note that **Region 7** can extend to $s > r_L + t_L$ should the use of an electromagnetic shield and isolation material be omitted.

Region		Boundaries	Description
1	Thermoplastic/Free Space	$0 \leq s < r_{ti}$	Desc.
2	Induction Target	$r_{ti} \leq s \leq r_{to}$	Desc.
3	Nozzle Housing (glass/ceramic)	$r_{to} < s < r_L - t_L/2$	Desc.
4	Driver Coil	$r_L - t_L/2 \leq s \leq r_L + t_L/2$	Desc.
5	Isolation Material	$r_L + t_L/2 < s < r_s$	Isolation material between Driver Coil and Electromagnetic Shield, could be .
6	Electromagnetic Shield	$r_s \leq s \leq r_s + t_s$	Desc.
7	Free Space	$r_s + t_s < s$	Desc.

3 Electromagnetics

This section outlines the derivation of a **continuous-time** solution to the electromagnetic field of the apparatus shown in **Figure 1**, for various driving frequencies and materials. While the effectiveness of this approach depends on several assumptions and approximations, (as opposed to a finite-element solution, which would not depend on any), it is useful as a computationally simple approach which models the electromagnetic response in a way that is useful for selecting both materials and driving/sensing electronics. Of particular note is that this model treats the electric and magnetic fields as if they were in $\hat{\phi}$ and $\hat{z}$ exclusively. A quick geometrical assessment, outlined in detail in **Appendix A.2**, shows that this is not *exactly* the case, due to the helical structure of the driver coil, but that this assumption has little consequence on the accuracy of this model, and is ignored henceforth. REMIND DEVOTED READERS THAT THESE

FIELD EQUATIONS ARE ¿¿¿ONLY¡¡¡ MEANT TO DERIVE THE FIELD INTENSITY IN and AROUND A SUFFICIENTLY EMBEDDED SECTION OF THE SOLENOID, SUCH AS THAT WHERE THE INDUCTION TARGET SHOULD BE.

3.1 Wave Propagation In Non-conductors

Field equations in material with no free charge, (essentially, air, vaccum, insulators/dielectrics such as glass/ceramics and poorly conducting plastics). Refraction does not occur at the boundaries because wave propagation is considered to be along $\hat{s}$exclusively in the region immediately around the target ring. GIVE REFERENCE FOR DERIVATION IN GRIFFITHS.

$$\left(\nabla^2 - \mu\epsilon\frac{\partial^2}{\partial t^2}\right)\vec{\mathbf{B}} = \vec{0} \qquad \left(\nabla^2 - \mu\epsilon\frac{\partial^2}{\partial t^2}\right)\vec{\mathbf{E}} = \vec{0} \tag{3.1}$$

Even though in a solenoid of finite length, the B field not necessarily uniform in $\hat{z}$ at the ends, the following is a reasonable approximation[1], due to the fact that the target ring is embedded a significant distance of the length of the coil in $\hat{z}$.

$$\vec{\mathbf{B}} = (0\hat{s} + 0\hat{\phi} + B_z(s,t)\hat{z}) \qquad \vec{\mathbf{E}} = (0\hat{s} + E_\phi(s,t)\hat{\phi} + 0\hat{z}) \tag{3.2}$$

Both $B_z(s,t)$ and $E_\phi(s,t)$ can be assumed to be of the form:

$$F(s,t) = S_F(s)T_F(t) = S_F(s)e^{iwt}$$

due to the fact that $\vec{\mathbf{B}}$ and $\vec{\mathbf{E}}$ propagate as plane waves. In cylindrical coordinates, (3.2) becomes:

$$\begin{aligned} \frac{1}{s}\frac{\partial B_z(s,t)}{\partial s} + \frac{\partial^2 B_z(s,t)}{\partial s^2} - \mu\epsilon\frac{\partial^2 B_z(s,t)}{\partial t^2} = 0 \\ \frac{1}{s}\frac{\partial E_\phi(s,t)}{\partial s} + \frac{\partial^2 E_\phi(s,t)}{\partial s^2} - \mu\epsilon\frac{\partial^2 E_\phi(s,t)}{\partial t^2} = 0 \end{aligned} \tag{3.3}$$

Since both $\vec{\mathbf{B}}$ and $\vec{\mathbf{E}}$ are plane waves, we can make the substitution, (with F representing either $B_z(s,t)$ or $E_\phi(s,t)$):

$$\frac{\partial^2 F(s,t)}{\partial t^2} = -\omega^2 F(s,t)$$

and then define the wave number $k = \frac{\omega}{c} = \omega\sqrt{\mu\epsilon}$. Both terms in (3.3) then take the form:

$$s^2\frac{\partial^2 F(s,t)}{\partial s^2} + s\frac{\partial F(s,t)}{\partial s} + s^2k^2F(s,t) = 0 \tag{3.4}$$

which is a Bessel Equation of Order Zero. The general solution of this equation is a superposition of Bessel functions of the first and second kind of order zero, (the full derivation can be found in [2], on page 292). The wave number, k, propagates through the derivation, and the result is:

$$F(s,t) = (c_1J_0(ks) + c_2Y_0(ks))e^{-iwt} \tag{3.5}$$

[1]Again, please refer to **Appendix A.2** for the particulars of why (3.2), while not rigorously accurate, is sufficient.

While the following is correct:

$$\begin{aligned} B_z(s,t) &= (c_1 J_0(ks) + c_2 Y_0(ks))e^{-iwt} \\ E_\phi(s,t) &= (c_3 J_0(ks) + c_4 Y_0(ks))e^{-iwt} \end{aligned} \tag{3.6}$$

it is not particularly useful as there are an excessive amount of variables to solve for with only two boundary conditions. However, $\vec{\mathbf{B}}$ and $\vec{\mathbf{E}}$ are coupled by Faraday's Law:

$$\nabla \times \vec{\mathbf{B}} = \mu_0 \epsilon_0 \frac{\partial \vec{\mathbf{E}}}{\partial t} + \mu_0 \vec{\mathbf{J}}$$

This, in cylindrical coordinates, and with the definition (3.2), can be rewritten as:

$$-\frac{\partial B_z(s,t)}{\partial s}\hat{\phi} = -\frac{i\omega}{c^2} E_\phi(s,t)\hat{\phi} + \mu_0 \vec{\mathbf{J}} \tag{3.7}$$

and since $\vec{\mathbf{J}} = \vec{\mathbf{0}}$ in a vaccuum:

$$E_\phi(s,t) = -\frac{ic^2}{\omega}\frac{\partial B_z(s,t)}{\partial s} \tag{3.8}$$

Differentiating J, (and also Y):

$$\begin{aligned} J_s^{(n)}(z) &= \frac{1}{2}\left(J_{s-1}^{(n-1)}(z) - J_{s+1}^{(n-1)}(z)\right) \\ J_{-n}(x) &= (-1)^n J_n(x) \end{aligned} \tag{3.9}$$

and applying it to (3.7):

$$E_\phi(s,t) = -\frac{ic^2}{\omega}\frac{k}{2}\left(c_1(J_{-1}(ks) - J_1 sk) + c_2(Y_{-1}(ks) - Y_1(ks))e^{-iwt}\right)$$

$$= -\frac{ic^2}{\omega}\frac{\omega}{2c}\left(c_1(-2J_1 ks) + c_2(-2Y_1(ks))e^{-iwt}\right)$$

and so, final solution for B, E in free space in cylindrical coords:

$$\begin{aligned} B_z(s,t) &= (c_1 J_0(ks) + c_2 Y_0(ks))e^{-iwt} \\ E_\phi(s) &= ic(c_1 J_1(ks) + c_2 Y_1(ks))e^{-iwt} \end{aligned} \tag{3.10}$$

Note that this final relation has only two unknowns to solve for, which allows for the simple solution of the coupled electromagnetic waves in a space with two defined boundary conditions. The consequences of this become apparent by the end of the section.

3.2 Wave Propagation In Conductor

Ampere's law the same. But entire Faraday's law now in effect. Applying Ohm's law:

$$\vec{\mathbf{J}} = \sigma\vec{\mathbf{E}}$$

Faraday's becomes:

$$\nabla \times \vec{\mathbf{B}} = \mu\sigma\vec{\mathbf{E}} + \mu\epsilon\frac{\partial\vec{\mathbf{E}}}{\partial t} \tag{3.11}$$

reference derivation in griffiths, changes (3.1) to:

$$\left(\nabla^2 - \mu\epsilon\frac{\partial^2}{\partial t^2} - \mu\sigma\frac{\partial}{\partial t}\right)\vec{\mathbf{B}} = \vec{0} \qquad \left(\nabla^2 - \mu\epsilon\frac{\partial^2}{\partial t^2} - \mu\sigma\frac{\partial}{\partial t}\right)\vec{\mathbf{E}} = \vec{0} \tag{3.12}$$

Again, using the definition of ∇^2 in clylindrical coordintes, as well as (3.2), these questions take the form of (3.3), but with an additional damping term:

$$\begin{aligned}
&\frac{1}{s}\frac{\partial B_z(s,t)}{\partial s} + \frac{\partial^2 B_z(s,t)}{\partial s^2} - \mu\epsilon\frac{\partial^2 B_z(s,t)}{\partial t^2} - \mu\sigma\frac{\partial B_z(s,t)}{\partial t} = 0 \\
&\frac{1}{s}\frac{\partial E_\phi(s,t)}{\partial s} + \frac{\partial^2 E_\phi(s,t)}{\partial s^2} - \mu\epsilon\frac{\partial^2 E_\phi(s,t)}{\partial t^2} - \mu\sigma\frac{\partial E_\phi(s,t)}{\partial t} = 0
\end{aligned} \tag{3.13}$$

Re-using the replacement of $E_\phi(s,t), B_z(s,t)$ with $F(s,t) = S_F(s)\cdot T_F(t)$, the pairs in (3.13) reduce to the following:

$$\frac{1}{s}\frac{\partial S_F(s)}{\partial s}T_F(t) + \frac{\partial^2 S_F(s)}{\partial s^2}T_F(t) - \mu\epsilon\frac{\partial^2 T_F(t)}{\partial t^2}S_F(s) - \mu\sigma\frac{\partial T_F(t)}{\partial t}S_F(s) = 0 \tag{3.14}$$

There seem to be two ways to go about solving this particular set of PDE's. The first method involves solving the separable differential equations by choosing a constant of integration, $-U^2$:

$$\begin{aligned}
&s^2\frac{\partial^2 S_F(s)}{\partial s^2} + s\frac{\partial S_F(s)}{\partial s} + U^2 S_F(s) = 0 \\
&\frac{\partial^2 T_F(t)}{\partial t^2} + \frac{\sigma}{\epsilon}\frac{\partial T_F(t)}{\partial t} + \frac{U^2}{\mu\epsilon}T_F(t) = 0
\end{aligned} \tag{3.15}$$

and then solving for $-U^2$ by choosing a solution for $T_F(t)$ that makes sense within this physical problem. The second method involves the quite reasonable assumption that, again, in the steady state, $T_F(t) = e^{-iwt}$. This follows a similar derivation method to the equations in a non-conductor, and (3.14) turns into:

$$s^2\frac{\partial^2 S_F(s)}{\partial s^2} + s\frac{\partial S_F(s)}{\partial s} + s^2(\mu\epsilon\omega^2 + i\mu\sigma\omega)S_F(s) = 0$$

The derivation for the first method is completely outlined in **Appendix A.1**. It turns out, that both methods result in the same set of answers:

$$U^2 = \mu\epsilon\omega^2 + i\mu\sigma\omega$$

$$F(s,t) = (c_1 J_0(Us) + c_2 Y_0(Us))e^{-iwt}$$

Then, applying the same methods to couple $\vec{\mathbf{B}}$ and $\vec{\mathbf{E}}$ that resulted in (3.10). Using (3.11):

$$\nabla \times \vec{\mathbf{B}} = \mu\sigma\vec{\mathbf{E}} + \mu\epsilon\frac{\partial\vec{\mathbf{E}}}{\partial t} == E_\phi(s,t)\cdot(\mu\sigma - i\mu\epsilon\omega) = E_\phi(s,t)\frac{U^2}{i\omega}$$

$$= -\frac{\partial B_z(s,t)}{\partial s} = U(c_1 J_1(U^2 s) + c_2 Y_1(U^2 s))e^{-iwt}$$

we arrive at the solution for cylindrical wave propagation in the conductor:

$$\begin{aligned} B_z(s,t) &= (c_1 J_0(U_{\mathcal{R}_i} s) + c_2 Y_0(U_{\mathcal{R}_i} s))e^{-iwt} \\ E_\phi(s) &= \frac{i\omega}{U_{\mathcal{R}_i}}(c_1 J_1(U_{\mathcal{R}_i} s) + c_2 Y_1(U_{\mathcal{R}_i} s))e^{-iwt} \end{aligned} \tag{3.16}$$

with a generic integration constant for region $\mathcal{R}_i$:

$$U^2_{\mathcal{R}_i} = \mu_{\mathcal{R}_i}\epsilon_{\mathcal{R}_i}\omega^2 + i\mu_{\mathcal{R}_i}\sigma_{\mathcal{R}_i}\omega \tag{3.17}$$

Now that all of the general solutions are defined, they can be applied across the operating regions to obtain a continuous-time solution for the field equations with a driving current of choice.

3.3 Generic Spatial Boundary Conditions

In dielectric regions, (**Regions 1,3,5,7**), both the electric and magnetic fields are considered to be continuous, and the boundary conditions are simply transfered from adjecent regions. A generic formulation of these conditions would look something like:

$$\begin{aligned} B_{i-1}(\partial\mathcal{R}_{i-1}\mathcal{R}_i) &= B_i(\partial\mathcal{R}_i\mathcal{R}_{i-1}), \qquad & B_i(\partial\mathcal{R}_i\mathcal{R}_{i+1}) &= B_{i+1}(\partial\mathcal{R}_i\mathcal{R}_{i+1}) \\ E_{i-1}(\partial\mathcal{R}_{i-1}\mathcal{R}_i) &= E_i(\partial\mathcal{R}_{i-1}\mathcal{R}_i), \qquad & E_i(\partial\mathcal{R}_i\mathcal{R}_{i+1}) &= E_{i+1}(\partial\mathcal{R}_i\mathcal{R}_{i+1}) \end{aligned} \tag{3.18}$$

where $\partial\mathcal{R}_i\mathcal{R}_j$ represents the boundary between region $\mathcal{R}_i$ and $\mathcal{R}_j$. However, because the fields are coupled, and there are values for both the electric and magnetic fields at the boundaries, in practice, only one set of boundary conditions is needed to solve for a particular region, with the second set becoming useful for solving for adjecent regions. As defined in **Table 2**, the only region that needs to be *defined* with two boundary conditions is $\mathcal{R}_4$. The remaining regions acquire boundary conditions as the solutions propagate through the model.

In conductors, (**Regions 2,4,6**), the coupling to adjecent regions, can also be defined as in

(3.18). However, for some situations, especially in the driver coil, where the driving current is defined, it can be advantageous to use enclosing boundary conditions for the fields and realize that they will both behave as functions of the enclosed current. This is dependent on one of the field equations:

$$I_{enc,\mathcal{R}_i} = \int_{\mathcal{V}_c} J_{\phi,\mathcal{R}_i}(\vec{r})d\tau = \int_{\mathcal{V}_c} \sigma E_{\phi,\mathcal{R}_i}(\vec{r})d\tau$$

where $\mathcal{V}_c$ is the conductor volume. At first, it may seem that this is a difficult integral to evaluate. Rigorous computational evaluation is likely best done by implementing a finite element scheme, which is not discussed here. Another interesting point is, that due to the fact that high driving frequencies are required to significantly heat the target in $\mathcal{R}_4$, ($\gtrsim$ 100kHz), there is a less computationally intensive approximation available taking into account the **skin depth**. The enclosed current is then, approximately, the electric field at the driving boundary multiplied by the conductance and the volume enclosed in the skin depth.

All conductors other than the driving solenoid, (discussed below), are treated as propagation regions with their own set of Bessel equations.

3.4 Boundary Conditions at the Driving Solenoid

The driving current in the primary coil is currently the only driving function for this model. It originates in **Region 4** , as defined in **Table 1**. It can be defined as a simple oscillator, with a respective phasor:

$$I(t) = I_{DC} + I_0(cos(\omega t)), \quad \mathbb{I}_0$$

or, if there are known harmonics present, (from, say, switching converter or PWM driver noise), as a Fourier series. However, if the occasional switching noise has a period much lower than that of the fundamental, or is properly filtered, it should only contribute the occasional transient response and will likely not factor in to the final inductance measurement. It is important to note this phemonenon however, because, while the driver current can likely be modelled to high accuracy in most cases, there exist situations where it may be critical, such as when high frequency induction measurements, or high percentile efficiency are required.

It is also important to note that the power transfer to the induction target is dependent on dI/dt only, and for maximum transfer, it is necessary to choose an I_{DC} such that $I_0 cos(\omega t$ spans the entire supply voltage without saturation. This is simple to implement with a standard PWM driver.

Due to the fact that the temperature sensing current is driven by a current mirror, and that the input phasor will effectively be constant in magnitude, the boosting effect of the coil on the magnetic field in all spatial regions can effectively be treated as a constant, which is superposed on any effects due to flux linkage. Using the definitions of retarted-time potentials, this can be derived in a finite length solenoid model for some frequency, at some height:

$$B_z(\omega, z)|_{\mathcal{R}_4^-} - B_z(\omega, z)|_{\mathcal{R}_4^+} = B_{\Delta Coil}(\omega, z) \tag{3.19}$$

Temperature sense current is a constant, because of current mirror type driver, so this *difference* always holds, no matter the specific values of internal/external fields due to flux linkage. This

can be coupled to the equation sets defined in (3.18):

$$B_{\mathcal{R}_3}(\delta\mathcal{R}_3\mathcal{R}_4^-) - B_{\mathcal{R}_5}(\delta\mathcal{R}_4\mathcal{R}_5^+) = B_{\Delta Coil}(\omega, z) \tag{3.20}$$

For now, however, it is convenient to use the infinite solenoid approximation, due to the fact that the height, h_L, is sufficiently larger than the nominal radius, r_L:

$$B_{\Delta Coil} \approx \mu \frac{I_{enc,\mathcal{R}_4}}{h_L} \tag{3.21}$$

and treat it as frequency independent, at least in the height region of the induction target, which is sufficiently embedded in the solenoid. The rigorous derivation of $B_{\Delta Coil}(\omega, z)$ is left for future versions.

3.5 Spatial Boundary Conditions for Full System Coupling

Using (3.10) and (3.16), the field equations across the model regions can be linked via the principles discussed in **Section 3.3** and the regions described in **Table 2**. Since there is a time-dependent e^{-iwt} component in every equation, these boundary solutions can be done with **phasor** values for the respective currents and voltages. Starting from the interior:

3.5.1 $\mathcal{R}_1$ to $\mathcal{R}_2$

Because J_1, Y_1 are singular at $s = 0$, they can be removed from the central region's solution.

B:

$$a_1 J_0(k_{\mathcal{R}_1} \cdot r_{ti}) = a_2 J_0(U_{\mathcal{R}_2} \cdot r_{ti}) + a_3 Y_0(U_{\mathcal{R}_2} \cdot r_{ti})$$

$$\boxed{0 = a_1 J_0(k_{\mathcal{R}_1} \cdot r_{ti}) - a_2 J_0(U_{\mathcal{R}_2} \cdot r_{ti}) - a_3 Y_0(U_{\mathcal{R}_2} \cdot r_{ti})} \tag{3.22}$$

E:

$$ic_{\mathcal{R}_1} a_1 J_1(k_{\mathcal{R}_1} \cdot r_{ti}) = \frac{i\omega}{U_{\mathcal{R}_2}}(a_2 J_1(U_{\mathcal{R}_2} \cdot r_{ti}) + a_3 Y_1(U_{\mathcal{R}_2} \cdot r_{ti}))$$

$$\boxed{0 = a_1 c_{\mathcal{R}_1} J_1(k_{\mathcal{R}_1} \cdot r_{ti}) - a_2 \frac{\omega}{U_{\mathcal{R}_2}} J_1(U_{\mathcal{R}_2} \cdot r_{ti}) - a_3 \frac{\omega}{U_{\mathcal{R}_2}} Y_1(U_{\mathcal{R}_2} \cdot r_{ti})} \tag{3.23}$$

3.5.2 $\mathcal{R}_2$ to $\mathcal{R}_3$

From here on, both Bessel functions are valid for all space and equation sets will look quite similar.

B:

$$a_2 J_0(U_{\mathcal{R}_2} \cdot r_{to}) + a_3 Y_0(U_{\mathcal{R}_2} \cdot r_{to}) = a_4 J_0(k_{\mathcal{R}_3} \cdot r_{to}) + a_5 Y_0(k_{\mathcal{R}_3} \cdot r_{to})$$

$$\boxed{0 = a_2 J_0(U_{\mathcal{R}_2} \cdot r_{to}) + a_3 Y_0(U_{\mathcal{R}_2} \cdot r_{to}) - a_4 J_0(k_{\mathcal{R}_3} \cdot r_{to}) - a_5 Y_0(k_{\mathcal{R}_3} \cdot r_{to})} \tag{3.24}$$

E:

$$\frac{i\omega}{U_{\mathcal{R}_2}}(a_2 J_1(U_{\mathcal{R}_2} \cdot r_{to}) + a_3 Y_1(U_{\mathcal{R}_2} \cdot r_{to})) = ic(a_4 J_1(k_{\mathcal{R}_3} \cdot r_{to}) + a_5 Y_1(k_{\mathcal{R}_3} \cdot r_{to}))$$

$$\boxed{0 = a_2 \frac{\omega}{U_{\mathcal{R}_2}} J_1(U_{\mathcal{R}_2} \cdot r_{to}) + a_3 \frac{\omega}{U_{\mathcal{R}_2}} Y_1(U_{\mathcal{R}_2} \cdot r_{to}) - a_4 c J_1(k_{\mathcal{R}_3} \cdot r_{to}) - a_5 c Y_1(k_{\mathcal{R}_3} \cdot r_{to})} \tag{3.25}$$

3.5.3 $\mathcal{R}_3$ to $\mathcal{R}_4$ to $\mathcal{R}_5$

The field equations near and inside $\mathcal{R}_4$ are somewhat complex to accurately solve for with a continuous-time model. While it is apparent that the majority of the current density, (and therefore, the highest amplitude electric field) will be near the conductors' surfaces, (as per the skin depth), this becomes complex to model near the Driver Coil as the conductor geometry is that of a circular wire, wound in a helix, and is not cylindrically symmetric or vertically homogeneous as it is presented here. Certainly in a finite-element model, this can be implemented in a more straightforward manner, but for now, a relatively accurate solution can be derived from caerfully defining some convenient boundary conditions around $\mathcal{R}_4$. Namely, that at the driver coil's internal boundaries, the magnetic field intensity is the standard $\mu NI/l_{coil}$, *and* that at both boundaries, due to the skin effect, the electric field intensity is identical, and proportianal to the current in the wire. Defining the following constants, for comfortable reading:

$$r_{IN} = r_L - \frac{t_L}{2}, \quad r_{OUT} = r_L - \frac{t_L}{2}$$

B:

$$B_z(r_{IN}) - B_z(r_{OUT}) = \mu \frac{I_{enc,\mathcal{R}_4}}{h_L}$$

$$B_z(r_{IN}) = a_4 J_0(k_{\mathcal{R}_3} \cdot r_{IN}) + a_5 Y_0(k_{\mathcal{R}_3} \cdot r_{IN})$$

$$B_z(r_{OUT}) = a_6 J_0(k_{\mathcal{R}_5} \cdot r_{OUT}) + a_7 Y_0(k_{\mathcal{R}_5} \cdot r_{OUT})$$

$$\boxed{\frac{\mu N_L \mathbb{I}_0}{h_L} = a_4 J_0(k_{\mathcal{R}_3} \cdot r_{IN}) + a_5 Y_0(k_{\mathcal{R}_3} \cdot r_{IN}) - a_6 J_0(k_{\mathcal{R}_5} \cdot r_{OUT}) - a_7 Y_0(k_{\mathcal{R}_5} \cdot r_{OUT})} \tag{3.26}$$

E:

$$ic_{\mathcal{R}_3}(a_4 J_1(k_{\mathcal{R}_3} \cdot r_{IN}) + a_5 Y_1(k_{\mathcal{R}_3} \cdot r_{IN})) = ic_{\mathcal{R}_5}(a_6 J_1(k_{\mathcal{R}_5} \cdot r_{OUT}) + a_7 Y_1(k_{\mathcal{R}_5} \cdot r_{OUT}))$$

$$\boxed{0 = a_4 J_1(k_{\mathcal{R}_3} \cdot r_{IN}) + a_5 Y_1(k_{\mathcal{R}_3} \cdot r_{IN}) - a_6 J_1(k_{\mathcal{R}_5} \cdot r_{OUT}) - a_7 Y_1(k_{\mathcal{R}_5} \cdot r_{OUT})} \tag{3.27}$$

3.5.4 $\mathcal{R}_5$ to $\mathcal{R}_6$

The next two sets are nearly identical to the sets around the target ring.

B:

$$a_6 J_0(k_{\mathcal{R}_5} \cdot r_{shi}) + a_7 Y_0(k_{\mathcal{R}_5} \cdot r_{shi}) = a_8 J_0(U_{\mathcal{R}_6} \cdot r_{shi}) + a_9 Y_0(U_{\mathcal{R}_6} \cdot r_{shi})$$

$$\boxed{0 = a_6 J_0(k_{\mathcal{R}_5} \cdot r_{shi}) - a_7 Y_0(k_{\mathcal{R}_5} \cdot r_{shi}) - a_8 J_0(U_{\mathcal{R}_6} \cdot r_{shi}) - a_9 Y_0(U_{\mathcal{R}_6} \cdot r_{shi})} \tag{3.28}$$

E:

$$ic_{\mathcal{R}_5}(a_6 J_1(k_{\mathcal{R}_5} \cdot r_{shi}) + a_7 Y_1(k_{\mathcal{R}_5} \cdot r_{shi})) = \frac{i\omega}{U_{\mathcal{R}_6}}(a_8 J_1(U_{\mathcal{R}_6} \cdot r_{shi}) + a_9 Y_1(U_{\mathcal{R}_6} \cdot r_{shi}))$$

$$\boxed{0 = a_6 c_{\mathcal{R}_5} J_1(k_{\mathcal{R}_5} \cdot r_{shi}) + a_7 c_{\mathcal{R}_5} Y_1(k_{\mathcal{R}_5} \cdot r_{shi}) - a_8 \frac{\omega}{U_{\mathcal{R}_6}} J_1(U_{\mathcal{R}_6} \cdot r_{shi}) - a_9 \frac{\omega}{U_{\mathcal{R}_6}} Y_1(U_{\mathcal{R}_6} \cdot r_{shi})} \tag{3.29}$$

3.5.5 $\mathcal{R}_6$ to $\mathcal{R}_7$

Conditions must be placed on the electromagnetic field equations which define that, in free space, they converge to a simple plane wave at $s \to \infty$, but that they are continuous at $\partial\mathcal{R}_6\mathcal{R}_7$. For this, it is convenient to use the definition of the Hankel function of the first kind, and its limit at $s \to \infty$ [3]:

$$H_0^{(1)}(x) = J_0(x) + iY_0(x)$$

$$\lim_{x\to\infty} H_0^{(1)}(x) = \sqrt{\frac{2}{\pi x}} e^{i(x-\pi/4)}$$

Then, using the familiar (3.8), and (3.9):

$$B_z(s) = c_1 H_0^{(1)}(ks)$$

$$E_\phi(s) = -\frac{ic^2}{\omega} c_1 \frac{\partial H_0^{(1)}(ks)}{\partial s}$$

$$\frac{\partial H_0^{(1)}(ks)}{\partial s} = \frac{\partial J_0(ks)}{\partial s}(J_0(ks) + iY_0(ks)) + i\frac{\partial Y_0(ks)}{\partial s}(J_0(ks) + iY_0(ks))$$

$$= \frac{\partial}{\partial s}\Big(J_0(ks) + iY_0(ks)\Big)(J_0(ks) + iY_0(ks)) = -k(J_1(ks) + iY_1(ks))(J_0(ks) + iY_0(ks))$$

$$E_\phi(s) = c_1 ic H_1^{(1)}(ks) H_0^{(1)}(ks)$$

Again, applying the relevant boundary conditions:

$$r_{SOUT} = r_{shi} + t_s$$

B:

$$a_8 J_0(U_{\mathcal{R}_6} \cdot r_{SOUT}) + a_9 Y_0(U_{\mathcal{R}_6} \cdot r_{SOUT}) = a_{10} H_0^{(1)}(k_{\mathcal{R}_7} \cdot r_{SOUT})$$

$$\boxed{0 = a_8 J_0(U_{\mathcal{R}_6} \cdot r_{SOUT}) + a_9 Y_0(U_{\mathcal{R}_6} \cdot r_{SOUT}) - a_{10} H_0^{(1)}(k_{\mathcal{R}_7} \cdot r_{SOUT})} \tag{3.30}$$

E:

$$\frac{i\omega}{U_{\mathcal{R}_6}}(a_8 J_1(U_{\mathcal{R}_6} \cdot r_{SOUT}) + a_9 Y_1(U_{\mathcal{R}_6} \cdot r_{SOUT})) = a_{10} i c_{\mathcal{R}_7} H_1^{(1)}(k_{\mathcal{R}_7} \cdot r_{SOUT}) H_0^{(1)}(k_{\mathcal{R}_7} \cdot r_{SOUT})$$

$$\boxed{\begin{array}{c} 0 = a_8 \frac{\omega}{U_{\mathcal{R}_6}} J_1(U_{\mathcal{R}_6} \cdot r_{SOUT}) + a_9 \frac{\omega}{U_{\mathcal{R}_6}} Y_1(U_{\mathcal{R}_6} \cdot r_{SOUT}) \dots \\ \\ \dots - a_{10} c_{\mathcal{R}_7} H_1^{(1)}(k_{\mathcal{R}_7} \cdot r_{SOUT}) H_0^{(1)}(k_{\mathcal{R}_7} \cdot r_{SOUT}) \end{array}} \tag{3.31}$$

Now that all possible spatial regions have been given a full set of boundary conditions, it is possible to solve the system.

4 Coupling Effects

Mathematics behind coupling of inudction target to driver coil as f(T,f). Mention that most of the math here is related to sensing, not driving currents. Due to superposition, they can be considered separately.

4.1 Transfer Matrices

The relationship between equations (3.22) to (3.31), can be defined in a transfer matrix, using the boundary conditions, $b_i \in \vec{b}$ to solve for coefficients, $a_i \in \vec{a}$. The standard transfer matrix with all regions from **Table 2** is defined in **Appendix B.4**.

$$\vec{b} = \mathbf{T}\vec{a}$$

Where, for example:

$$\vec{b} = \mathbf{T}\vec{a}$$

4.2 Back EMF in Driving Coil

Over the height of the target, ($z \in \{d_0, d_0 + h_T\}$), the field equations will take on different values at the boundaries of $\mathcal{R}_4$ than at other values of z due to the flux linkage expressed in the transfer matrices. Across all temperatures, the flux linkage with the coil and the electromagnetic shield at all other heights is considered to be constant.

The temperature dependent EMF, $V_T(\Delta T, \omega)$, from the induction target can be defined across the driver coil by integrating the complex-valued electric field around however many loops happen to have their geometries in $z \in \{d_0, d_0 + h_T\}$. The actual EMF is the largest value integral of any line which is monotonically increasing in Z which also passes in the $d\vec{A}$ direction inside the helical conductor geometry. This can be done helically, for a more accurate impedance value, but it is likely sufficient to just integrate once over each circular loop and then sum the contributions from loops at heights throughout $z \in \{d_0, d_0 + h_T\}$. It is important to note that this is not an exact integration along $\vec{\mathbf{J}}_L$ but in some line which approximately follows $\vec{\mathbf{J}}_L$ in the coil to produce an EMF across it.

MAYBE INCLUDE A LITTLE PICTURE ILLUSTRATION HERE, LATER

Definition, where Γ_i is a circular loop in coil winding $i \in \{1, 2, \ldots, n\}$ out of n coil windings in $z \in \{d_0, d_0 + h_T\}$, for some temperature change $\Delta T = T_2 - T_1$:

$$V_T(\Delta T, \omega) = \sum_{i=1}^{n} \left(\max \left(\int_{\Gamma_i} \vec{\mathbf{E}}(T_2, \omega, s(\Gamma_i(\phi))) \cdot \vec{dl} \right) \ldots \right.$$
$$\left. \ldots - \max \left(\int_{\Gamma_i} \vec{\mathbf{E}}(T_1, \omega, s(\Gamma_i(\phi))) \cdot \vec{dl} \right) \right) \tag{4.1}$$

and, from derivations in **Section 3.5.3**, and the fact that the largest field is somewhere on the

surface of each coil due to the skin effect. Since the field is the same at the inner and outer radius, pick r_{OUT} for larger integral value:

$$V_T(\Delta T, \omega) \approx 2\pi r_{OUT} \cdot n \cdot (E_\phi(T_2, \omega, r_{OUT}) - E_\phi(T_1, \omega, r_{OUT})) \tag{4.2}$$

5 Simluation

Plots of resultant system responses w.r.t various operating schema, (from POV of equation variables).

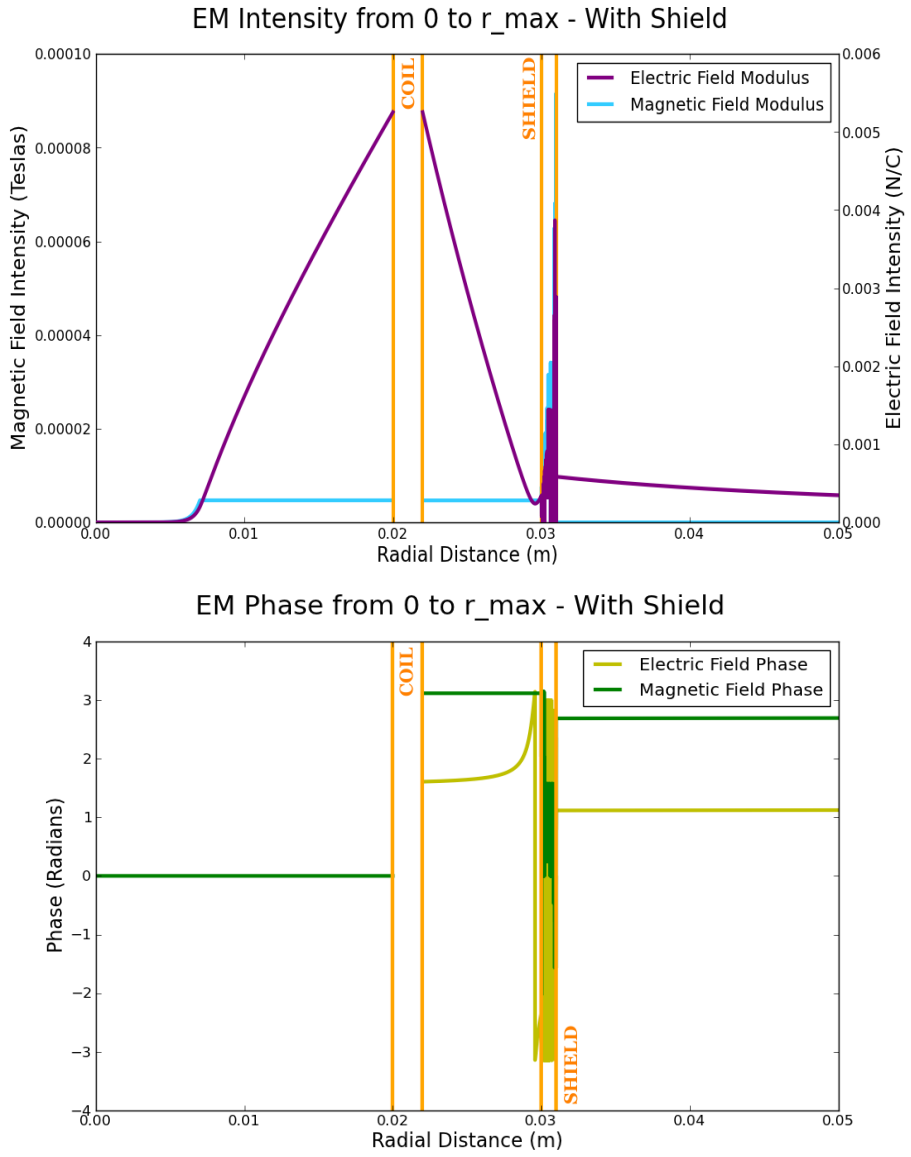

Figure 2: Steady state EM field solution for complete model defined in **Appendix B.4**. solution, (computed w/ SciPy 0.10.0), given some realistic spatial/material parameters. The model is likely subject to severe floating point arithmetic error in the shield region, where the Bessel functions start to take on large, ($> 10^{200}$) values. **Section 4**). It is peculiar that the Hankel function solutions outside this region do not experience the same effects.

6 Implementation

6.1 Electronic Interface

High level, (non specific, eg. block diagrams) outline of possible implementation schema from an electronic POV).

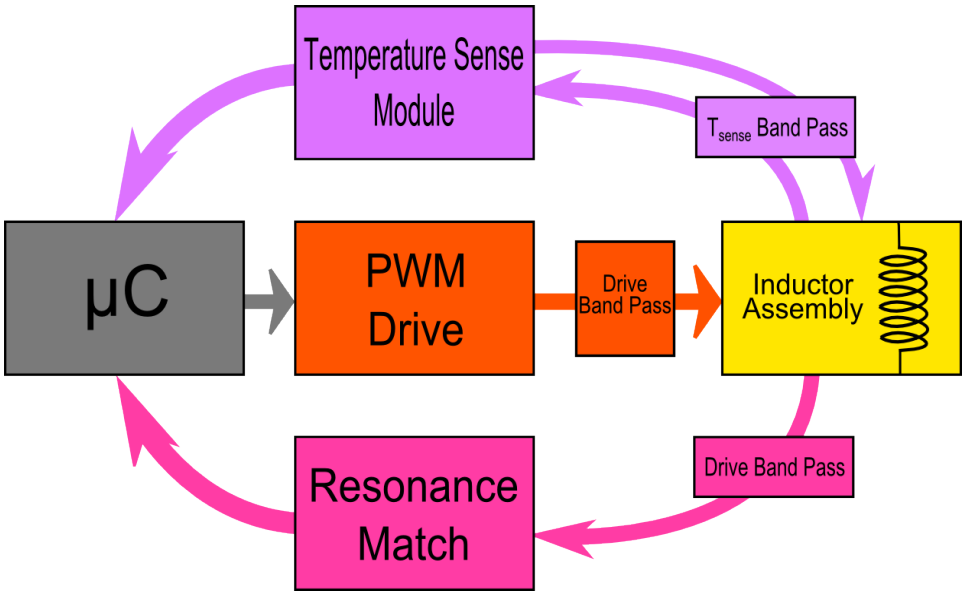

Figure 3: High level block diagram of a possible control system for the inductive load. This model revolves around two basic mechanisms: matching resonance in the inductive load for maximum power transfer, and an isolated T_{sense} current to sense inductor impedance, (when calibrated properly, this is a reliable method of sensing the temperature of the induction target, as per mechanisms discussed in **Section 4**).

6.2 Inductor Assembly Materials

7 Implementation - Materials

This section will deal with various implementation schema and materials used and explain how they effect operational parameters.

8 Conclusion

Concludes presented information and points towards future developments.

Acknowledgements

References

[1] David J. Griffiths, *Introduction to Electrodynamics*. Prentice Hall Inc., New Jersey, 1999.

[2] William E. Boyce, *Elementary Differential Equations and Boundary Value Problems*. John Wiley and Sons Inc., New Jersey, 2009.

[3] J. D. Templin, *Exact solution to the field equations in the case of an ideal infinite solenoid*. American Journal of Physics, **63** (10) 1995. 916-919

A Supplementary Derivations

A.1 Derivation of $T_F(t)$ for Fields in Conductor

The first approach for deriving the modified wave number constant, U, is simply solving for $T_F(t)$ as shown in, (3.15). The characteristic equation for the separable PDE for $T_F(t)$ is:

$$\mu\epsilon r^2 + \mu\sigma r + U^2 = 0$$

Finding the roots:

$$r = \frac{-\sigma}{2\epsilon} \pm \sqrt{\left(\frac{\sigma}{2\epsilon}\right)^2 - \frac{U^2}{\mu\epsilon}}$$

Now, by definition of electromagnetic waves, the time varying solution *m*ust be an oscillator. Keeping this in mind, then, the final solution must be of the form:

$$T_F(t) = g(t) \cdot e^{-i\omega t}$$

Then, making a convenient factorization in r:

$$r = \frac{-\sigma}{2\epsilon} \pm i\sqrt{\frac{U^2}{\mu\epsilon} - \left(\frac{\sigma}{2\epsilon}\right)^2}$$

However, simply using the value for r defined above leads to a problem. Let the solution to the PDE, using r as is, be:

$$T_F(t)' = e^{\frac{-\sigma}{2\epsilon}t} \cdot (c_1 e^{i\omega' t} + c_2 e^{-i\omega' t})$$

with

$$\omega' = \sqrt{\frac{U^2}{\mu\epsilon} - \left(\frac{\sigma}{2\epsilon}\right)^2}$$

This is clearly an issue because it suggests that, regardless of the, certainly, time-dependent boundary conditions in the induction target region, that:

$$\lim_{t\to\infty} T_F(t)' = 0$$

While this may make sense for a transient response, it is implied from the operation of this model that the current in the Driver Coil is alternating and, via Faraday's Law, continually inducing an alternating current in the induction target. This explicitly prevents the field intensity from permanently decaying. To rectify the solution for $T_F(t)$, a value for U^2 is chosen such that *a*t least one of the roots does not have a real component.

$$\mathrm{Re}\{r_2\} = \mathrm{Re}\left\{\frac{-\sigma}{2\epsilon} - i\sqrt{\frac{U^2}{\mu\epsilon} - \left(\frac{\sigma}{2\epsilon}\right)^2}\right\} = 0$$

This implies that:

$$\frac{-\sigma}{2\epsilon} - i\sqrt{\frac{U^2}{\mu\epsilon} - \left(\frac{\sigma}{2\epsilon}\right)^2} = -i\omega$$

Which, after some simple arithmetic, yields:

$$U^2 = \mu\epsilon\omega^2 + i\mu\sigma\omega$$

$$r_1 = \frac{-\sigma}{\epsilon} + i\omega$$

The complete solution for the time dependence is then:

$$T_F(t) = c_1 e^{-i\omega t} + c_2 e^{\frac{-\sigma}{\epsilon}t} e^{i\omega t}$$

In steady state operation, the decaying portion of $T_F(t)$ dissapears, so selecting a value of 0 for c_2 is within reason. Finally, then, the solution becomes:

$$T_F(t) = c_1 e^{-i\omega t}$$

where c_1 can be absorbed in the constants of $S_F(s)$. The value for U^2 matches the value derived in **Section 3.2**, and confirms that the assumption that $T_F(t)$ is a simple plane wave in $\hat{s}$ is reasonable.

A.2 Realistic Field Orientation

In reality, $\vec{\mathbf{E}}$ and $\vec{\mathbf{B}}$ are *not* exclusively in $\hat{\phi}$ and $\hat{z}$, as defined in **Figure 1**, due to the fact that the wire thickness in the solenoid is *not* zero. The voltage across the coil is the primary driver of current and the corresponding electric field points in the ϕ' direction, which can be defined as:

$$\hat{\phi}' = \frac{1}{\sqrt{1 + \left(\frac{h_{turn}}{2\pi r_{nom}}\right)^2}} \left(\hat{\phi} + \frac{h_{turn}}{2\pi r_{nom}}\hat{z}\right)$$

where h_{turn} is the nominal height of a single helical loop in the coil. If the separation between wires is near zero, (and for maximum internal field strength, it should be), then $h_{turn} \approx t_L$. It can also be said that

$$\frac{\vec{\mathbf{J}}_L}{\left|\vec{\mathbf{J}}_L\right|} = \hat{\phi}'$$

Similarly, the magnetic field is in an axis $\hat{z}'$ orthogonal to $\hat{\phi}'$, but in the $z\phi$ plane:

$$\hat{z}' = \frac{1}{\sqrt{1 + \left(\frac{h_{turn}}{2\pi r_{nom}}\right)^2}} \left(-\frac{h_{turn}}{2\pi r_{nom}}\hat{\phi} + \hat{z}\right)$$

However, in the majority of practical applications of this model, where $h_{turn} \approx t_L <<< r_{nom}$, this has only a slight effect on the inductive mechanics of the system. The slight axial component of the electric field will induce a small dipole moment across any interior conductors, and the slight angular component of the magnetic field will result in as lower axial field intensity and, by Ampere's law, a small reduction in induced current in both the primary winding and interior

conductor(s). Certainly the induced dipole moment in an alternating field has the capability of adding additional thermal excitation to the target. While these effects are present, and may warrant further examination in cases where large sensitivity and peculiar conductor geometries are a concern, they are not discussed here in detail.

A.3 Absence of an Electromagnetic Shield or Target

Removing either, or both the electromagnetic shield and the induction target from the system simply involves defining a new set of boundary conditions around the driver coil. Using the following definitions for the three subsequent derivations:

$$r_{IN} = r_L - \frac{t_L}{2}, \quad r_{OUT} = r_L - \frac{t_L}{2}$$

$$B_z(r_{IN}) - B_z(r_{OUT}) = \mu \frac{I_{enc,\mathcal{R}_4}}{h_L}$$

A.3.1 Absence of Target

Considering the nozzle material and interior free space separately:

B:

$$a_1 J_0(k_{\mathcal{R}_1} \cdot r_{to}) = a_4 J_0(k_{\mathcal{R}_3} \cdot r_{to}) + a_5 Y_0(k_{\mathcal{R}_3} \cdot r_{to}) \tag{A.1}$$

$$\boxed{0 = a_1 J_0(k_{\mathcal{R}_1} \cdot r_{to}) - a_4 J_0(k_{\mathcal{R}_3} \cdot r_{to}) - a_5 Y_0(k_{\mathcal{R}_3} \cdot r_{to})} \tag{A.2}$$

E:

$$ic_{\mathcal{R}_1} a_1 J_1(k_{\mathcal{R}_1} \cdot r_{to}) = ic_{\mathcal{R}_3}(a_4 J_1(k_{\mathcal{R}_3} \cdot r_{to}) + a_5 Y_1(k_{\mathcal{R}_3} \cdot r_{to})$$

$$\boxed{0 = c_{\mathcal{R}_1} a_1 J_1(k_{\mathcal{R}_1} \cdot r_{to}) - c_{\mathcal{R}_3} a_4 J_1(k_{\mathcal{R}_3} \cdot r_{to}) - c_{\mathcal{R}_3} Y_1(k_{\mathcal{R}_3} \cdot r_{to})} \tag{A.3}$$

OR, if the speed of wave propagation in the nozzle material and interior free space is approximately identical, then they can be blended into one dielectric region. The "field boosting" boundary condition around the coil still remains:

B:

$$B_z(r_{IN}) = a_1 J_0(k \cdot r_{IN}) \tag{A.4}$$

$$B_z(r_{OUT}) = a_6 J_0(k \cdot r_{OUT}) + a_7 Y_0(k \cdot r_{OUT})$$

$$\boxed{\frac{\mu N_L \mathbb{I}_0}{h_L} = a_1 J_0(k \cdot r_{IN}) - a_6 J_0(k \cdot r_{OUT}) - a_7 Y_0(k \cdot r_{OUT})} \tag{A.5}$$

E:

$$ica_1 J_1(k \cdot r_{IN}) = ic(a_6 J_1(k \cdot r_{OUT}) + a_7 Y_1(k \cdot r_{OUT}))$$

$$\boxed{0 = a_1 J_1(k \cdot r_{IN}) - a_6 J_1(k \cdot r_{OUT}) - a_7 Y_1(k \cdot r_{OUT})} \tag{A.6}$$

A.3.2 Absence of Electromagnetic Shield

B:

$$B_z(r_{IN}) = a_4 J_0(k \cdot r_{IN}) + a_5 Y_0(k \cdot r_{IN})$$

$$B_z(r_{OUT}) = a_{10} H_0^{(1)}(k \cdot r_{OUT})$$

$$\boxed{\frac{\mu N_L \mathbb{I}_0}{h_L} = a_4 J_0(k \cdot r_{IN}) + a_5 Y_0(k \cdot r_{IN}) - a_{10} H_0^{(1)}(k \cdot r_{OUT})} \tag{A.7}$$

E:

$$ic(a_4 J_1(k \cdot r_{IN}) + a_5 Y_1(k \cdot r_{IN})) = ica_{10} H_1^{(1)}(k \cdot r_{OUT}) H_0^{(1)}(k \cdot r_{OUT})$$

$$\boxed{0 = a_4 J_1(k \cdot r_{IN}) + a_5 Y_1(k \cdot r_{IN}) - a_{10} H_1^{(1)}(k \cdot r_{OUT}) H_0^{(1)}(k \cdot r_{OUT})} \tag{A.8}$$

A.3.3 Absence of Both

The following assumes blended interior regions.

B:

$$B_z(r_{IN}) = a_1 J_0(k \cdot r_{IN})$$

$$B_z(r_{OUT}) = a_{10} H_0^{(1)}(k \cdot r_{OUT})$$

$$\boxed{\frac{\mu N_L \mathbb{I}_0}{h_L} = a_1 J_0(k \cdot r_{IN}) - a_{10} H_0^{(1)}(k \cdot r_{OUT})} \tag{A.9}$$

E:

$$ica_1 J_1(k \cdot r_{IN}) = ica_{10} H_1^{(1)}(k \cdot r_{OUT}) H_0^{(1)}(k \cdot r_{OUT})$$

$$\boxed{0 = a_1 c_{\mathcal{R}_1} J_1(k \cdot r_{IN}) - a_{10} c_{\mathcal{R}_7} H_1^{(1)}(k \cdot r_{OUT}) H_0^{(1)}(k \cdot r_{OUT})} \tag{A.10}$$

The absence of both the target and shield geometry greatly simplifies the system.

B Transfer Matrices

B.1 Shield-Less, Target-Less, Single Dielectric, Transfer Matrix

$$\vec{b} = \mathbf{T}\vec{a}, \quad r_{IN} = r_L - \frac{t_L}{2}, \quad r_{OUT} = r_L - \frac{t_L}{2}, \quad \vec{b} = \begin{bmatrix} \frac{\mu N_L \mathbb{I}_0}{h_L} \\ 0 \end{bmatrix}, \quad \vec{a} = \begin{bmatrix} a_1 \\ a_{10} \end{bmatrix}$$

$$\mathbf{T} = \begin{bmatrix} J_0(k \cdot r_{IN}) & -H_0^{(1)}(k \cdot r_{OUT}) \\ c_{\mathcal{R}_1} J_1(k \cdot r_{IN}) & -c_{\mathcal{R}_7} H_1^{(1)}(k \cdot r_{OUT}) H_0^{(1)}(k \cdot r_{OUT}) \end{bmatrix} \tag{B.1}$$

B.2 Target-Less Transfer Matrix

$$\vec{b} = \mathbf{T}\vec{a}, \quad r_{IN} = r_L - \frac{t_L}{2}, \quad r_{OUT} = r_L - \frac{t_L}{2}, \quad r_{SOUT} = r_{shi} + t_s \quad \vec{b} = \begin{bmatrix} \frac{\mu N_L \mathbb{I}_0}{h_L} \\ 0 \\ 0 \\ 0 \\ 0 \\ 0 \end{bmatrix}, \quad \vec{a} = \begin{bmatrix} a_1 \\ a_6 \\ a_7 \\ a_8 \\ a_9 \\ a_{10} \end{bmatrix}$$

$$\mathbf{T} = \begin{bmatrix} J_0(k_{\mathcal{R}_1} \cdot r_{IN}) & -J_0(k_{\mathcal{R}_5} \cdot r_{OUT}) & -Y_0(k_{\mathcal{R}_5} \cdot r_{OUT}) & 0 & 0 & 0 \\ c_{\mathcal{R}_1} J_1(k_{\mathcal{R}_1} \cdot r_{IN}) & -c_{\mathcal{R}_5} J_1(k_{\mathcal{R}_5} \cdot r_{OUT}) & -c_{\mathcal{R}_5} Y_1(k_{\mathcal{R}_5} \cdot r_{OUT}) & 0 & 0 & 0 \\ 0 & J_0(k_{\mathcal{R}_5} \cdot r_{shi}) & Y_0(k_{\mathcal{R}_5} \cdot r_{shi}) & -J_0(U_{\mathcal{R}_6} \cdot r_{shi}) & -Y_0(U_{\mathcal{R}_6} \cdot r_{shi}) & 0 \\ 0 & c_{\mathcal{R}_5} J_1(k_{\mathcal{R}_5} \cdot r_{shi}) & c_{\mathcal{R}_5} Y_1(k_{\mathcal{R}_5} \cdot r_{shi}) & -\frac{\omega}{U_{\mathcal{R}_6}} J_1(U_{\mathcal{R}_6} \cdot r_{shi}) & -\frac{\omega}{U_{\mathcal{R}_6}} Y_1(U_{\mathcal{R}_6} \cdot r_{shi}) & 0 \\ 0 & 0 & 0 & J_0(U_{\mathcal{R}_6} \cdot r_{SOUT}) & Y_0(U_{\mathcal{R}_6} \cdot r_{SOUT}) & -H_0^{(1)}(k_{\mathcal{R}_7} \cdot r_{SOUT}) \\ 0 & 0 & 0 & \frac{\omega}{U_{\mathcal{R}_6}} J_1(U_{\mathcal{R}_6} \cdot r_{SOUT}) & \frac{\omega}{U_{\mathcal{R}_6}} Y_1(U_{\mathcal{R}_6} \cdot r_{SOUT}) & -c_{\mathcal{R}_7} H_1^{(1)}(k_{\mathcal{R}_7} \cdot r_{SOUT}) H_0^{(1)}(k_{\mathcal{R}_7} \cdot r_{SOUT}) \end{bmatrix} \tag{B.2}$$

B.3 Shield-Less Transfer Matrix

$$\vec{b} = \mathbf{T}\vec{a}, \quad r_{IN} = r_L - \frac{t_L}{2}, \quad r_{OUT} = r_L - \frac{t_L}{2}, \quad \vec{b} = \begin{bmatrix} 0 \\ 0 \\ 0 \\ 0 \\ \frac{\mu N_L \mathbb{I}_0}{h_L} \\ 0 \end{bmatrix}, \quad \vec{a} = \begin{bmatrix} a_1 \\ a_2 \\ a_3 \\ a_4 \\ a_5 \\ a_{10} \end{bmatrix}$$

$$\mathbf{T} = \begin{bmatrix} J_0(k_{\mathcal{R}_1} \cdot r_{ti}) & -J_0(U_{\mathcal{R}_2} \cdot r_{ti}) & -Y_0(U_{\mathcal{R}_2} \cdot r_{ti}) & 0 & 0 & 0 \\ c_{\mathcal{R}_1} J_1(k_{\mathcal{R}_1} \cdot r_{ti}) & -\frac{\omega}{U_{\mathcal{R}_2}} J_1(U_{\mathcal{R}_2} \cdot r_{ti}) & -\frac{\omega}{U_{\mathcal{R}_2}} Y_1(U_{\mathcal{R}_2} \cdot r_{ti}) & 0 & 0 & 0 \\ 0 & J_0(U_{\mathcal{R}_2} \cdot r_{to}) & Y_0(U_{\mathcal{R}_2} \cdot r_{to}) & -J_0(k_{\mathcal{R}_3} \cdot r_{to}) & -Y_0(k_{\mathcal{R}_3} \cdot r_{to}) & 0 \\ 0 & \frac{\omega}{U_{\mathcal{R}_2}} J_1(U_{\mathcal{R}_2} \cdot r_{to}) & \frac{\omega}{U_{\mathcal{R}_2}} Y_1(U_{\mathcal{R}_2} \cdot r_{to}) & -c_{\mathcal{R}_3} J_1(k_{\mathcal{R}_3} \cdot r_{to}) & -c_{\mathcal{R}_3} Y_1(k_{\mathcal{R}_3} \cdot r_{to}) & 0 \\ 0 & 0 & 0 & J_0(k_{\mathcal{R}_3} \cdot r_{IN}) & Y_0(k_{\mathcal{R}_3} \cdot r_{IN}) & -H_0^{(1)}(k_{\mathcal{R}_7} \cdot r_{OUT}) \\ 0 & 0 & 0 & c_{\mathcal{R}_3} J_1(k_{\mathcal{R}_3} \cdot r_{IN}) & c_{\mathcal{R}_3} Y_1(k_{\mathcal{R}_3} \cdot r_{IN}) & -c_{\mathcal{R}_7} H_1^{(1)}(k_{\mathcal{R}_7} \cdot r_{SOUT}) H_0^{(1)}(k_{\mathcal{R}_7} \cdot r_{SOUT}) \end{bmatrix} \tag{B.3}$$

B.4 Complete Transfer Matrix

$$\vec{b} = \mathbf{T}\vec{a}, \qquad \begin{matrix} r_{IN} = r_L - \frac{t_L}{2} \\ r_{SOUT} = r_{shi} + t_s \end{matrix} \qquad \begin{matrix} r_{OUT} = r_L - \frac{t_L}{2} \\ - \end{matrix}, \qquad \begin{matrix} \vec{b} = \begin{bmatrix} 0 & 0 & 0 & 0 & \frac{\mu N_L \mathbb{I}_0}{h_L} & 0 & 0 & 0 & 0 & 0 \end{bmatrix}^T \\ \vec{a} = \begin{bmatrix} a_1 & a_2 & a_3 & a_4 & a_5 & a_6 & a_7 & a_8 & a_9 & a_{10} \end{bmatrix}^T \end{matrix}$$

$$\mathbf{T} = \begin{bmatrix} J_0(k_{\mathcal{R}_1} \cdot r_{ti}) & -J_0(U_{\mathcal{R}_2} \cdot r_{ti}) & -Y_0(U_{\mathcal{R}_2} \cdot r_{ti}) & 0 & 0 \\ c_{\mathcal{R}_1} J_1(k_{\mathcal{R}_1} \cdot r_{ti}) & -\frac{\omega}{U_{\mathcal{R}_2}} J_1(U_{\mathcal{R}_2} \cdot r_{ti}) & -\frac{\omega}{U_{\mathcal{R}_2}} Y_1(U_{\mathcal{R}_2} \cdot r_{ti}) & 0 & 0 \\ 0 & J_0(U_{\mathcal{R}_2} \cdot r_{to}) & Y_0(U_{\mathcal{R}_2} \cdot r_{to}) & -J_0(k_{\mathcal{R}_3} \cdot r_{to}) & -Y_0(k_{\mathcal{R}_3} \cdot r_{to}) \\ 0 & \frac{\omega}{U_{\mathcal{R}_2}} J_1(U_{\mathcal{R}_2} \cdot r_{to}) & \frac{\omega}{U_{\mathcal{R}_2}} Y_1(U_{\mathcal{R}_2} \cdot r_{to}) & -c_{\mathcal{R}_3} J_1(k_{\mathcal{R}_3} \cdot r_{to}) & -c_{\mathcal{R}_3} Y_1(k_{\mathcal{R}_3} \cdot r_{to}) \\ 0 & 0 & 0 & J_0(k_{\mathcal{R}_3} \cdot r_{IN}) & Y_0(k_{\mathcal{R}_3} \cdot r_{IN}) \\ 0 & 0 & 0 & c_{\mathcal{R}_3} J_1(k_{\mathcal{R}_3} \cdot r_{IN}) & c_{\mathcal{R}_3} Y_1(k_{\mathcal{R}_3} \cdot r_{IN}) \\ 0 & 0 & 0 & 0 & 0 \\ 0 & 0 & 0 & 0 & 0 \\ 0 & 0 & 0 & 0 & 0 \\ 0 & 0 & 0 & 0 & 0 \end{bmatrix}$$

$$\begin{bmatrix} 0 & 0 & 0 & 0 & 0 \\ 0 & 0 & 0 & 0 & 0 \\ 0 & 0 & 0 & 0 & 0 \\ 0 & 0 & 0 & 0 & 0 \\ -J_0(k_{\mathcal{R}_5} \cdot r_{OUT}) & -Y_0(k_{\mathcal{R}_5} \cdot r_{OUT}) & 0 & 0 & 0 \\ -c_{\mathcal{R}_5} J_1(k_{\mathcal{R}_5} \cdot r_{OUT}) & -c_{\mathcal{R}_5} Y_1(k_{\mathcal{R}_5} \cdot r_{OUT}) & 0 & 0 & 0 \\ J_0(k_{\mathcal{R}_5} \cdot r_{shi}) & Y_0(k_{\mathcal{R}_5} \cdot r_{shi}) & -J_0(U_{\mathcal{R}_6} \cdot r_{shi}) & -Y_0(U_{\mathcal{R}_6} \cdot r_{shi}) & 0 \\ c_{\mathcal{R}_5} J_1(k_{\mathcal{R}_5} \cdot r_{shi}) & c_{\mathcal{R}_5} Y_1(k_{\mathcal{R}_5} \cdot r_{shi}) & -\frac{\omega}{U_{\mathcal{R}_6}} J_1(U_{\mathcal{R}_6} \cdot r_{shi}) & -\frac{\omega}{U_{\mathcal{R}_6}} Y_1(U_{\mathcal{R}_6} \cdot r_{shi}) & 0 \\ 0 & 0 & J_0(U_{\mathcal{R}_6} \cdot r_{SOUT}) & Y_0(U_{\mathcal{R}_6} \cdot r_{SOUT}) & -H_0^{(1)}(k_{\mathcal{R}_7} \cdot r_{SOUT}) \\ 0 & 0 & \frac{\omega}{U_{\mathcal{R}_6}} J_1(U_{\mathcal{R}_6} \cdot r_{SOUT}) & \frac{\omega}{U_{\mathcal{R}_6}} Y_1(U_{\mathcal{R}_6} \cdot r_{SOUT}) & -c_{\mathcal{R}_7} H_1^{(1)}(k_{\mathcal{R}_7} \cdot r_{SOUT}) H_0^{(1)}(k_{\mathcal{R}_7} \cdot r_{SOUT}) \end{bmatrix} \tag{B.4}$$